Comparison of Thermodynamic Retrieval by the Adjoint Method with the Traditional Retrieval Method

JUANZHEN SUN AND N. ANDREW CROOK

National Center for Atmospheric Research, Boulder, Colorado*

(Manuscript received 6 December 1994, in final form 11 July 1995)

ABSTRACT

The adjoint technique for retrieval of the thermodynamic fields is compared with the traditional technique of Gal-Chen and Hane. The comparison is performed using both Doppler radar observations and simulated data. The real dataset is a gust-front case observed during the Phoenix II experiment. The simulated data are from a numerical experiment of a collapsing cold pool. In the simulated data study, we assume that observations of the horizontal velocity are available, either from a dual-Doppler synthesis or from a single-Doppler retrieval. Tests are performed on data that have been degraded in various ways to replicate real data. These tests include the sensitivity to the temporal sampling frequency, random error, spatially correlated error, and divergent/rotational error in the forcing terms. In most of the cases examined, it is found that the adjoint method is able to retrieve the buoyancy field more accurately than the traditional technique.

1. Introduction

Remote sensing of the atmosphere by Doppler radars is increasing substantially at present. The WSR-88D network, when completed, will provide nearly complete coverage over the United States, while Terminal Doppler Weather Radars (TDWR) are being installed at 45 major airports around the country. The measurements provided by these platforms are generally limited to reflectivity and radial velocity. A number of methods have been proposed recently to derive the cross-beam velocity components. The most obvious technique is to deploy a second Doppler radar with a different viewing angle (dual Doppler). A variant on this method is to deploy just a receiver and to take bistatic measurements (Wurman 1994). Other techniques rely on the assumption that reflectivity (or radial velocity) acts as a tracer in the flow and hence can be tracked to determine the flow field. These methods include statistical techniques such as TREC (tracking reflectivity echoes by correlation; Tuttle and Foote 1990) and methods based on an equation for reflectivity conservation (Qiu and Xu 1992; Laroche and Zawadsky 1993; Shapiro et al. 1994; Gal-Chen and Zhang 1993; Xu et al. 1993).

With the deployment of these new observing platforms and the development of techniques to estimate the cross-beam velocity, it is reasonable to expect that high-resolution datasets of horizontal velocity will soon be available in many areas. If these datasets are to be used in numerical models, then it will be necessary to obtain corresponding datasets of the mass (or temperature) field. However, there is no current observing technique that can provide temperature fields with comparable spatial and temporal resolution.

This lack of detailed temperature observations has led researchers to examine methods for *retrieving* the temperature field from observations of the velocity field. The early work in thermodynamic retrieval was pioneered by Gal-Chen (1978) and Hane and Scott (1978). These researchers showed that the pressure and temperature deviation from horizontal average fields could be retrieved from velocity observations. If absolute values of pressure and temperature are needed in the observed volume, an independent measurement of either temperature or pressure is needed in a single column somewhere in the analysis volume. This technique, which we will herein call the traditional technique, has been applied to numerous observational cases as well as simulated data cases (Hane et al. 1981; Gal-Chen and Kropfli 1984; Parsons et al. 1987; Crook 1994; to mention but a few). A modification of the Gal-Chen and Hane technique was given by Roux (1985) by including a simplified thermodynamic equation to find total rather than perturbation thermodynamic fields.

Rapid development of the adjoint method for fitting a numerical model to observational data has been seen in recent years. The adjoint formalism was first proposed by Le Dimet (1982) for meteorological appli-

* The National Center for Atmospheric Research is sponsored by the National Science Foundation.

Corresponding author address: Dr. Juanzhen Sun, NCAR/MMM Division, P.O. Box 3000, Boulder, CO 80307-3000.

cations and was then implemented by Derber (1985), Courtier (1985), Le Dimet and Talagrand (1986), Talagrand and Courtier (1987), Courtier and Talagrand (1990), and Zou et al. (1993a, 1993b), among others. To date, most applications of the adjoint method have been to fit a numerical model with certain dependent variables to observations of all the dependent variables. However, as shown by Sun et al. (1991), the adjoint method can also be used to retrieve unobserved variables. In Sun et al. (1991) and Sun and Crook (1994), the cross-beam velocity components and temperature were retrieved from observations of radial velocity and reflectivity in the boundary layer from a single-Doppler radar. Although the extension of the technique to observations from dual-Doppler radars is quite straightforward, the performance of the adjoint technique in thermodynamic retrieval has never been compared to the traditional technique.

It should be noted that both the traditional technique and the adjoint technique are not limited to thermodynamic retrieval. Microphysical retrieval using moist models has also been attempted (Rutledge and Hobbs 1983; Ziegler 1985; Hauser and Amayenc 1986; Verlinde and Cotton 1993; Sun et al. 1995). In this paper, however, we restrict our study to the dry boundary layer. Or in other words, we assume velocity observations are from clear-air echoes. Wilson and Schreiber (1986) have pointed out the importance of low-level convergence lines in initiating thunderstorms. They found that 80% of the thunderstorms in the Denver area formed along radar-detected boundaries. Boundary layer winds also have a significant impact on airport operations and safety. Methodologies for forecasting low-level winds have been developed by a number of researchers, including numerical prediction using a small-scale model (Crook and Tuttle 1994; Crook and Cole 1994). One of the key elements in the numerical prediction of low-level winds is the successful determination of the initial temperature field.

In the present study, we compare the performance of the traditional technique with that of the adjoint method in retrieving the buoyancy field in the boundary layer. We compare these two techniques by first using dual-Doppler observations from the Phoenix II experiment and then using simulated data of a collapsing cold pool. We use simulated data in some of these tests so as to provide a baseline for comparison. Since the traditional technique requires the availability of two Cartesian horizontal velocity components (though not the adjoint technique as will be shown in section 2) before the thermodynamic retrieval is performed, in the simulated data study, both methods use the two Cartesian velocity components as observations. By doing so, we focus our present study on the comparison of these two techniques in thermodynamic retrieval given analyzed velocity data. In the real data study, however, the adjoint technique assimilates the radial velocities directly, while a velocity synthesis is performed to obtain the Cartesian horizontal velocity components for the traditional technique.

The outline of the present study is as follows. In section 2, we describe the traditional thermodynamic retrieval technique as well as the adjoint method. In section 3, we compare these two techniques using data of a gust front observed during the Phoenix II experiment. In the first part of section 4, we describe the control simulation of a collapsing cold pool and test the retrieval algorithms on "perfect" data. In the second part of section 4, we apply both techniques to simulated data that has been degraded in some way. We first compare and contrast the performance of the two techniques on data that are error-free but with temporal resolutions similar to the expected operational resolution. We then compare their performance on data that has various forms of error added to it. The conclusions are given in section 5.

2. Thermodynamic retrieval

The numerical model used in this study is the dry, Boussinesq model of Sun et al. (1991). The momentum, thermodynamic, and continuity equations are

$$\frac{d\mathbf{v}}{dt} - \delta_{i3}\frac{g\theta}{\Theta_0}\mathbf{k} + \nabla p - \nu\nabla^2\mathbf{v} = 0, \tag{2.1}$$

$$\frac{d\theta}{dt} + w\frac{\partial\Theta}{\partial z} - \kappa\nabla^2\theta = 0, \tag{2.2}$$

$$\nabla\cdot\mathbf{v} = 0. \tag{2.3}$$

Here $\mathbf{v}$ is the velocity vector, p is the perturbation pressure divided by a reference density, θ is the perturbation potential temperature, Θ is the horizontal mean potential temperature, and Θ_0 is the reference potential temperature. The quantity ν is the eddy viscosity and κ is the thermal diffusivity which are both assumed constant.

a. Traditional method

To describe the traditional thermodynamic retrieval technique, we first write the two horizontal momentum equations in the form

$$F = -p_x,$$
$$G = -p_y, \tag{2.4}$$

where $[F, G]$ include the acceleration and mixing terms. The first step in the traditional technique is to determine the terms $[F, G]$ from the velocity data $[u, v, w]$. If the retrieval is being performed over N grid points, then (2.4) represents $2N$ equations for N variables, namely the pressure p. Thus, the system (2.4) is overdetermined and will only have a solution if $F_y = G_x$ (the vertical vorticity equation). Because of errors in the data and/or model, generally, $F_y \neq G_x$. We therefore search for the pressure that minimizes the re-

siduals of (2.4) over the domain of interest, that is, the minimum of

$$\iint[(F + p_x)^2 + (G + p_y)^2]dxdy. \quad (2.5)$$

This can be done by solving the Euler equation

$$\frac{\partial^2 p}{\partial x^2} + \frac{\partial^2 p}{\partial y^2} = \frac{\partial F}{\partial x} + \frac{\partial G}{\partial y}, \quad (2.6a)$$

subject to the boundary conditions,

$$F = -p_x \quad \text{at } x \text{ boundaries},$$
$$G = -p_y \quad \text{at } y \text{ boundaries}. \quad (2.6b)$$

As described by Gal-Chen (1978), (2.6a) can be solved up to a horizontal constant. This constant can be determined if an independent measurement of either temperature or pressure in a single column exists (e.g., from a sounding) somewhere in the domain of interest.

A common practice in retrieval studies is to use the "momentum checking" parameter E_r as a measure of the performance of the retrieval. [Other measures of performance suggested by Gal-Chen and Kropfli (1984) are time continuity and physical plausability.] Parameter E_r is given by

$$E_r = \frac{\iint(F + p_x)^2 + (G + p_y)^2 dxdy}{\iint(F^2 + G^2)dxdy}. \quad (2.7)$$

However, some care must be exercised when interpreting E_r as a measure of the accuracy of the retrieval. This can be illustrated by separating $[F, G]$ into the "true" component $[F_t, G_t]$, which balances the true pressure, p_t, that is,

$$F_t = -(p_t)_x,$$
$$G_t = -(p_t)_y, \quad (2.8)$$

and an error $[F_e, G_e]$. The error can be further split into a divergent component $[F_d, G_d]$ and a rotational component $[F_r, G_r]$, that is,

$$F = F_t + F_d + F_r,$$
$$G = G_t + G_d + G_r, \quad (2.9)$$

where $[F_d, G_d] = [\phi_x, \phi_y]$ and $[F_r, G_r] = [\psi_y, -\psi_x]$. It is important to note that we are referring to divergent/rotational error in the term $[F, G]$ and not in the velocity fields.

If the error is purely divergent, that is, $F = F_t + \phi_x$ and $G = G_t + \phi_y$, then (2.4) becomes

$$(p_t)_x + \phi_x = -p_x,$$
$$(p_t)_y + \phi_y = -p_y. \quad (2.10)$$

Equation (2.8) has been used in obtaining (2.10). It is seen that, for this special case, (2.4) can be satisfied exactly, and the resultant pressure will be

$$p = -p_t - \phi. \quad (2.11)$$

Furthermore, the momentum checking value E_r will vanish even though there exists error in the data and the retrieved buoyancy.

If the error in $[F, G]$ is purely rotational then the right-hand side of (2.6a) is unchanged. As long as no error is added to the boundary conditions, then the true pressure, p_t, will be recovered. The momentum checking value for this case will be

$$E_r = \frac{\iint(\psi_y)^2 + (\psi_x)^2 dxdy}{\iint(F^2 + G^2)dxdy}. \quad (2.12)$$

Hence, $E_r \neq 0$ even though the pressure is recovered exactly. The above analysis has indicated that some caution needs to be exercised when interpreting the value of E_r obtained in a particular retrieval. For this reason we suggest that other measures of performance, such as time continuity and physical plausability, should also be used in conjuction with momentum checking when evaluating the performance of a retrieval.

In section 4d we will compare the performance of the two retrieval methods in handling divergent and rotational errors in $[F, G]$. The terms $[F, G]$ include a tendency term (linear with respect to $[u, v]$), advection terms (nonlinear), and a simple diffusion term (linear). As will be shown, it is simplest to add divergent/rotational error through the tendency terms since this can be achieved by adding divergent/rotational error directly to the velocity fields.

Once the pressure has been retrieved, the buoyancy field can be determined from the vertical equation of motion, which is written as

$$H = -p_z + B, \quad (2.13)$$

where H includes the acceleration and mixing term and B represents the buoyancy.

On an Arakawa C grid (Arakawa and Lamb 1977), the w field and hence the variable H are located between the pressure and buoyancy levels. Equation (2.13) is thus discretized in the vertical as

$$H^{k+1/2} = -\frac{(p^{k+1} - p^k)}{dz} + \frac{(B^{k+1} + B^k)}{2}$$

"exact" method. (2.14)

If simulated data is being used, and if one wishes to recover the exact buoyancy field, then it is necessary to sum from the top or bottom boundary starting with the buoyancy at that boundary. This we will call the

"exact" method [(2.14)]. If error exists in the data, then this summation procedure tends to lead to noisy buoyancy fields. An alternative procedure, which we call the "inexact" method [(2.15)], is to calculate the buoyancy by centered differencing the pressure over $2\Delta z$, that is,

$$\frac{(H^{k+1/2} + H^{k-1/2})}{2} = -\frac{(p^{k+1} - p^{k-1})}{2dz} + B^k \quad \text{"inexact" method.} \quad (2.15)$$

Although the exact buoyancy field cannot be recovered with this procedure when error-free data is used, it does substantially reduce the noise in the buoyancy field when data *with* error is used.

b. Adjoint method

The aim of the adjoint method is to find the initial buoyancy field that gives a model trajectory that fits the data with minimum error. A cost function is thus defined to measure the difference between the observations and the model solution.

In this study, two cost functions are employed depending on the form of the input data. If the data are in the form of horizontal velocity components, the cost function J_1 is given by

$$J_1 = \sum_T \sum_\sigma [(u - u^{ob})^2 + (v - v^{ob})^2] + \text{P1} + \text{P2}, \quad (2.16)$$

where T and σ denote the temporal and spatial domains, respectively, $[u, v]$ are model solutions of the horizontal velocity, and the quantities with the superscript "ob" represent their observations.

The last two terms in the cost function, P1 and P2, represent penalty functions. Here P1 is the smoothness penalty function defined by

$$\text{P1} = \sum_T \sum_\sigma \rho_1(\delta_{tt}\theta)^2 + \rho_2[(\delta_{xx}\theta)^2 + (\delta_{yy}\theta)^2] + \rho_3(\delta_{zz}\theta)^2, \quad (2.17)$$

where the quantities ρ_1, ρ_2, and ρ_3 are penalty constants that determine the weights assigned to the smoothness constraints. For the experiments presented in this paper, the value of 0.05 is used for the three constants. Term δ_{tt} denotes the second-order finite difference in time, that is

$$\delta_{tt}\theta = \theta^{n+1} - 2\theta^n + \theta^{n-1}, \quad (2.18)$$

where n represents the nth time level. The second-order finite differences in space, δ_{xx}, δ_{yy}, and δ_{zz} are defined in a similar way. The smoothness constraint can also be enforced on the velocity fields. However, since the observations of these fields provides adequate information, the effect of the penalty functions for these fields is negligible. If the observations contains substantially large errors, however, the use of the smoothness penalty for velocity fields will generally be helpful in suppressing noise.

A stability penalty function, P2, is imposed to restrict the development of static instability in the solution. Penalty function P2 is given by

$$\text{P2} = \begin{cases} \sum_T \sum_\sigma [\rho_4(\theta_{k+1} - \theta_k)^2], & \theta_{k+1} < \theta_k \\ 0, & \theta_{k+1} \geqslant \theta_k, \end{cases} \quad (2.19)$$

where k refers to the vertical level and ρ_4 is the penalty constant set to 0.05 in this study.

A second cost function, J_2, is defined when the input data are radial velocity observations. It is given by

$$J_2 = \sum_T \sum_\sigma [(v_{r1} - v_{r1}^{ob})^2 + (v_{r2} - v_{r2}^{ob})^2] + \text{P1}, \quad (2.20)$$

The quantities v_{r1}^{ob} and v_{r2}^{ob} represent radial velocity observations from two different radars and v_{r1} and v_{r2} are their model counterparts calculated using the model velocity components (u, v, w) using the following relation:

$$v_r = u\frac{x - x_0}{r} + v\frac{y - y_0}{r} + w\frac{z - z_0}{r}, \quad (2.21)$$

where r is the distance between a radar location (x_0, y_0, z_0) and a grid point (x, y, z).

The independent, or control, variables in the cost functions J_1 or J_2 are the initial conditions of u, v, w, and θ. Their values at any later time can be obtained by integrating the model equations. If we have perfect observations of the velocity fields, they can be directly inserted into the model as initial conditions. In this case, the buoyancy is the only control parameter, and we can define the following variational problem: find the buoyancy trajectory that is the solution of the model equations (2.1) – (2.3) that minimizes the cost function J. This is a constrained minimization problem with the model equations representing the constraint. It should be noted that when large errors are contained in the velocity observations, it is better to treat the velocity fields as control variables so that a best-fitted initial state can be defined. If radial velocity observations are used as input, that is, the cost function J_2 is minimized, the velocity fields must be treated as control variables. The minimization is performed using Nocedal's limited memory, a quasi-Newton conjugate gradient algorithm VA15AD (Liu and Nocedal 1988). This minimization requires knowledge of the gradients of the cost function with respect to the control variables. These gradients are computed by backward integrating a set of time-dependent equations, the adjoint equations.

The procedure for retrieving the buoyancy field using the adjoint method can be summarized as follows.

(i) Choose a first guess for the control variables.

(ii) Integrate the model to obtain the trajectory of the dynamic variables to be used in the calculation of the cost function and the integration of the adjoint model.

(iii) Calculate the cost function.

(iv) Calculate the gradient of the cost function with respect to the control variables by integrating the adjoint equations backward.

(v) Determine the search direction and the step size and then find a new estimate of the control variables toward the minimum of the cost function using the calculated cost function and its gradient.

(vi) Check if a satisfactory solution has been found. If not, the above procedure can be repeated using the new values of the control variables as a new first guess and continue the process until a satisfactory solution is determined.

The derivation of the adjoint equations was given in Sun et al. (1991); the reader is referred to that paper for details. The search direction and the step size in (v) are automatically computed in the minimization algorithm VA15AD as long as the values of the cost function and the gradient are supplied. Their detailed computation procedure is not given here. Interested readers are referred to Liu and Nocedal (1988) or Gill et al. (1981) for a review of minimization algorithms. To compute the step size in (v), the algorithm may require that the cost function and its gradient be calculated more than one time for each iteration. We will refer to the number of times the cost function and its gradient are computed as the number of simulations throughout this paper. Since for most iterations the step size can be found by calculating the cost function and its gradient once, the number of simulations and the number of iterations are quite close. Because two integrations, forward model integration and adjoint model integration, have to be performed for each simulation, the cost of one simulation is about two to three times the cost of an integration of the numerical model over the assimilation period.

To summarize, both the traditional and the adjoint thermodynamic retrieval attempt to find the buoyancy field that is the solution of a set of governing equations, given a time history of the observations of the velocity fields. To achieve this goal, however, the adjoint method uses a different approach from the traditional method. In the traditional method, the buoyancy field is calculated from the governing equations using the velocity observations. The observations are inserted into the model equations directly or after a least squares fit in time. In contrast, the adjoint method finds the solution of the buoyancy field from the governing equations by iteratively minimizing a cost function defined by the difference between the solution of the governing equations and the observations. By doing so, an optimal solution, which satisfies the model and fits the data as close as possible, is obtained. Given velocity fields at the start and the end of the assimilation window, the concepts for both methods are illustrated and compared in Fig. 1. The two black dots represent the velocity data at the start ($t = 0$) and the end ($t = T$) of the assimilation window, which are some distance away from the model trajectory (or the true atmospheric trajectory) represented by the solid curve due to errors in observation and in analysis. For the traditional retrieval, the tendency terms are calculated by finite difference using data at $t = 0$ and $t = T$, which is equivalent to assuming a linear evolution in the time window $[0, T]$ as illustrated by the dot–dashed curve. In general, this trajectory will not be a solution of the model equation, and hence the momentum checking value will be nonzero. With the tendency terms computed in this fashion, the buoyancy field at a point between $t = 0$ and $t = T$ can be determined given the calculated values of the advection and mixing terms at that point. For the adjoint technique, a time evolution represented by the dashed curve can be obtained by adjusting the initial state to minimize the difference between model solutions and data. The buoyancy field at any point between $t = 0$ and $t = T$ is given by integrating the model equations starting from the resultant optimal initial state. The time evolution obtained using the adjoint technique is optimal in that it is the one closest to observations and yet satisfies the model. (By definition the momentum checking value is zero for this solution.) If the optimal solution is uniquely defined and the model evolution is not linear, we expect that the buoyancy field obtained using the adjoint method will be more accurate.

3. Comparison using real data

The observations used in this section were collected during the Phoenix II experiment, conducted in 1984

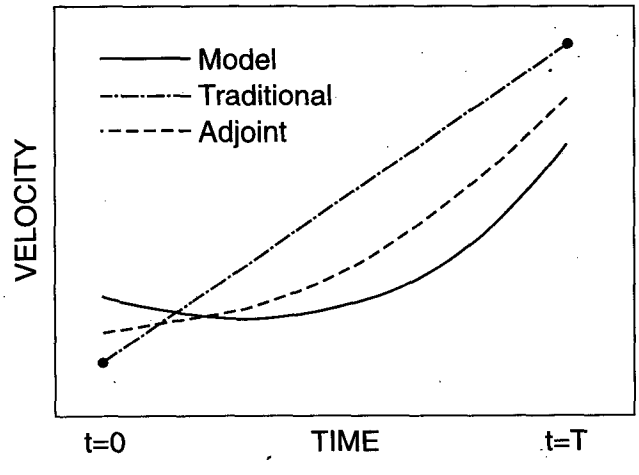

FIG. 1. Illustration of fitting a model to data by the traditional method and the adjoint method. The solid curve represents the model trajectory. The black dots represent data at the start and the end of the assimilation window.

on the High Plains of eastern Colorado. Two X-band Doppler radars observed a 60° segment of space centered on the same point. The radial velocity and reflectivity were recorded by both radars at an interval of about 2 min.

The gust front to be examined occurred during the afternoon of 19 June 1984. This gust front was formed by evaporative cooling from an earlier thunderstorm. As described by Mueller and Carbone (1987), this gust front initiated several storms as it moved to the northwest at a speed of approximately 7 m s^{-1}. Both sounding and mesonet observations showed a 2.5°C temperature drop as the gust front passed through. Sun and Crook (1994) have used this dataset in a study of wind and thermodynamic retrieval by the adjoint technique assuming observations from only one radar were available. In this paper, we will use observations from both radars to examine the thermodynamic retrieval and compare it with the traditional technique.

Several processing steps were applied to the Doppler measurements to obtain gridded radial velocity data. The processing methods were described in Sun and Crook (1994). These gridded radial velocity data were then used as input in the cost function J_2 for the adjoint technique. For the traditional technique, a Doppler synthesis must be performed to produce the horizontal velocity components u and v to be used in the thermodynamic retrieval. Although the adjoint technique can also use the synthesized u and v as input, it is preferable to use the direct observations so as to keep the data as much intact as possible. Being able to use the direct observations is in fact an advantage of the adjoint technique over the traditional technique.

Four volumes of gridded radial velocity data and synthesized horizontal velocity data were derived at 2229:30, 2231:20, 2233:10, and 2235:00 UTC. The retrieval experiments were performed with the temporal window between 2229:30 and 2235:00 UTC. For the adjoint retrieval, we conducted experiments using four volumes of data and two volumes of data, respectively, and the results showed little sensitivity to the number of data volumes used. Figure 2a displays the retrieved perturbation potential temperature field at z = 100 m and at t = 2232:30 UTC (middle of the assimilation window) for the experiment using two volumes of data (2229:30 and 2235:00 UTC) in the adjoint retrieval. As can be seen from the figure, the retrieval has produced cold air behind the leading edge of the gust front. Although a direct comparison can not be made with the surface observation, since the retrieved buoyancy is the average over the lowest grid box (200 m), we are encouraged that the retrieved maximum temperature deficit of 1.8°C is of a similar magnitude to the observed surface temperature drop of 2.5°C.

For the traditional technique, we ran three experiments to test the sensitivity of the thermodynamic retrieval to the method used to calculate the time-derivative terms. In the first experiment, we computed the

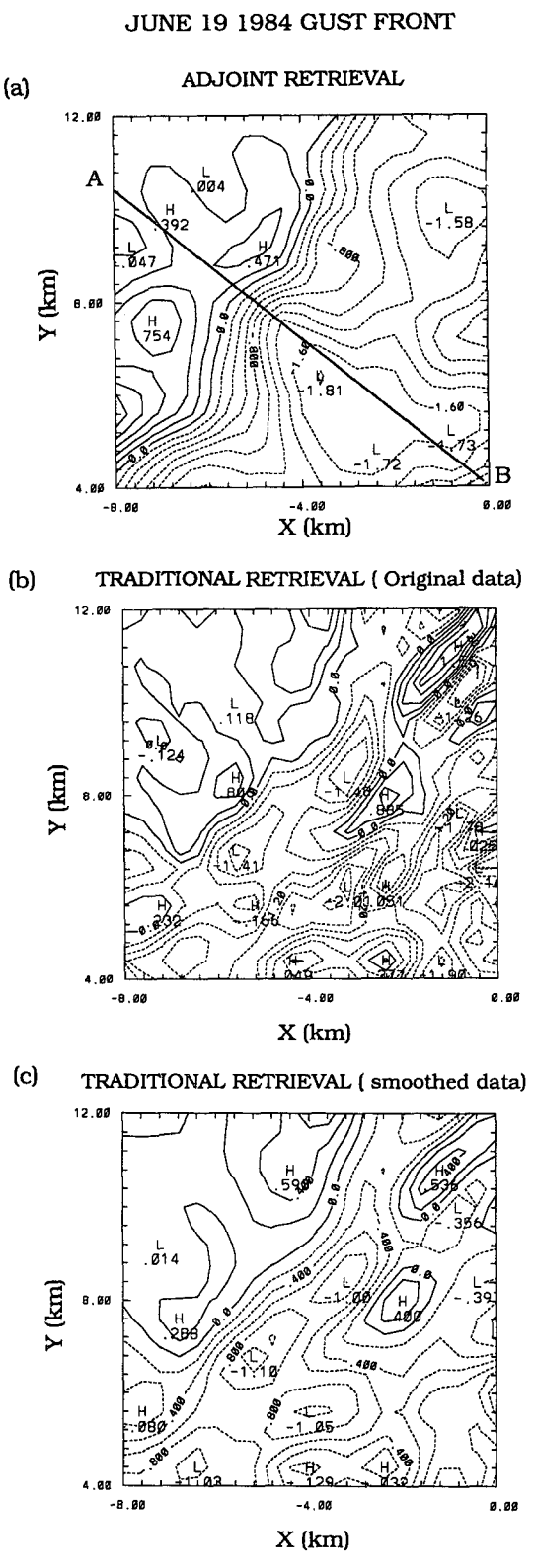

FIG. 2. Retrieved θ field at z = 100 m and t = 2232:30 UTC for the 19 June 1984 gust front using (a) the adjoint technique, (b) the traditional technique with the original synthesized data, and (c) the traditional technique with the smoothed data.

tendency terms by using the velocity data at the start (2229:30 UTC) and the end (2235:00 UTC) of the time window. The advection and mixing terms were calculated using their average. In experiment 2, the tendency terms were estimated by a linear least squares fit using the four volumes of data. The third experiment was similar to the second, except that a quadratic fitting was performed. The retrieved buoyancy fields from these three experiments showed similar characteristics, although some small-scale differences appeared. The retrieved perturbation potential temperature fields from the first experiment using the original synthesized data and the smoothed data are shown in Figs. 2b and 2c, respectively. The momentum checking value was 0.4 for the original data and 0.31 for the smoothed data. Comparing Figs. 2b and 2c with Fig. 2a, we observe that the retrievals using the traditional technique are rather noisy even after considerable smoothing is applied to the velocity data. The well-organized gust-front structure presented in the adjoint retrieval is not clearly shown in the traditional retrieval. The air behind the gust front in the traditional retrieval is less cold than in the adjoint retrieval. Furthermore, regions of positive buoyancy have also been retrieved in the cold pool.

Figure 3 shows the vertical cross section of the retrieved potential temperature field through line *AB* indicated in Fig. 1a from the adjoint retrieval and the traditional retrieval (smoothed data). The contour shows the potential temperature subtracted by 300°C. A well-defined gust front can be seen in the boundary layer in the adjoint retrieval. In the traditional retrieval, however, some small-scale regions of warm air are present in the cold air behind the gust front.

The above comparison suggests that the adjoint technique works better in eliminating noise while retaining the signal of the gust front. With real data, a quantitative comparison of these two technique is impossible because we do not have temperature observations with the same resolution as the velocity data. For this reason, we will make comparison of these two technique using simulated data in the next section.

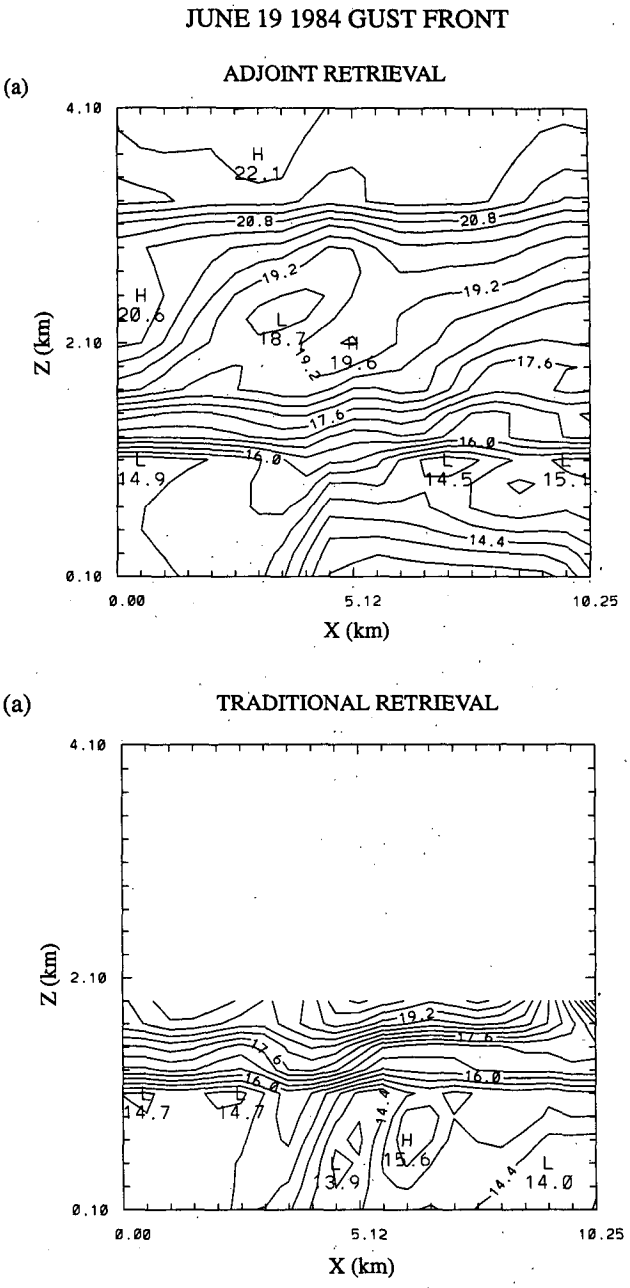

FIG. 3. Vertical cross section of the retrieved perturbation potential temperature field at t = 2232:30 UTC through line *AB* indicated in Fig. 2a using (a) the adjoint technique and (b) the traditional technique. The contour values shown in the figure are subtracted by 300°C.

4. Comparison using simulated data

a. Control experiment and testing of retrieval schemes

The control experiment in this section is a simulation of a collapsing cold pool. We choose this particular flow because it is both simple and often observed on the mesoscale. This experiment was also used in Crook (1994), so that comparison can be made with the results from that study. The simulation was run on a domain of 39 km in the horizontal and 4.2 km in the vertical. The grid spacing was 1 km in the horizontal and 0.2 km in the vertical. The basic state of the atmosphere was neutral with the mean potential temperature of 300°C. The simulation commenced with a cylindrical cold pool of 10-km radius and 2-km depth given by

$$\theta = 3.0\,\frac{e^{(r-r_w)/r_w} - e^{(r-r_w)/r_w}}{e^{(r-r_w)/r_w} + e^{(r-r_w)/r_w}}, \qquad (2.22)$$

which yields a maximum perturbation potential temperature of −2.3°C. In (2.22), r_w represents the width

of the cylindrical cold pool and r is the distance from the center of the cold pool.

The simulation was run for 25 min, with lateral boundary conditions of zero normal velocities and zero fluxes for the other variables. The time step was 15 s. The horizontal velocity fields, u and v, from the control simulation were stored as observations. The retrieval experiments were conducted on a domain of 33 km $\times$ 33 km $\times$ 4.2 km. We carefully selected the dimension of the domain and the size and strength of the initial perturbation so that the cold air remained in the domain away from the lateral boundaries.

Figure 4 shows the perturbation potential temperature and velocity field at $t = 20$ min in a vertical cross section through the center of the cold pool. The horizontal velocity is 11 m s^{-1} behind the leading edges of the cold pool. The maximum values of the updraft and downdraft are around 1.8 m s^{-1}.

We first tested the schemes on "perfect" data, namely data that were error-free and available at every time step. The initial test for the traditional method was performed using the velocity fields at three adjacent time levels (19.75, 20, and 20.25 min). The tendency terms were calculated by differencing the data at $t = 19.75$ min and $t = 20.25$ min. The advection and mixing terms were calculated using data at $t = 20$ min. We also assumed that the mean state sounding was taken just inside the northwest corner of the domain (the reason for choosing this location will be explained in section 4b). Using these data, the "exact" method should be able to retrieve the buoyancy within the machine accuracy. Indeed, with this method, the perturbation potential temperature was retrieved to an accuracy of 10^{-8} °C (rms error), suggesting that the retrieval algorithm had been coded correctly. When the "inexact" method was used, the rms error in the retrieved θ field was 0.02°C, or 8% if measured by the relative rms error (the rms error normalized by the rms buoyancy).

For the adjoint method, it is important to check if the gradient obtained by the integration of the adjoint model is correct. One way to perform the verification of the gradient is to compare it with the finite-difference approximation of the gradient (Sun et al. 1991). Results suggested that the gradient calculation by the adjoint model was correct.

An initial test for the adjoint method was conducted using data at every time level between $t = 17.5$ min and $t = 22.5$ min, starting with the initial guess of zero buoyancy and "observed" velocities. Since the solution procedure of the adjoint method is iterative, the accuracy of the solution depends on the number of iterations. Obtaining a retrieved θ field with an accuracy of the order of 10^{-8} °C, as in the above, is almost impossible. However, we were able to obtain an accuracy similar to the "inexact" method (8% relative rms error) after 100 iterations using the adjoint method.

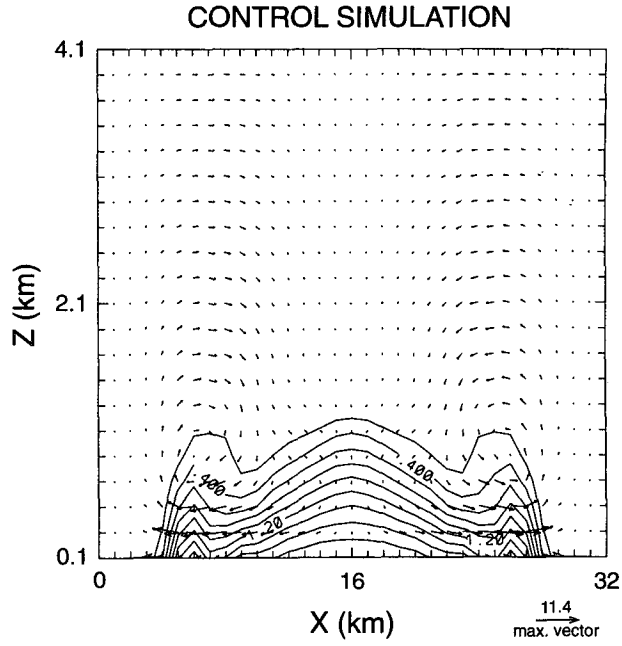

FIG. 4. Perturbation potential temperature θ and velocity vector in a vertical cross section through the center of the cold pool at $t = 20$ min from the control simulation. The contour interval is 0.2°C. Solid lines are used for negative θ contours and dashed lines are used for positive contours.

Another test with the adjoint method was performed to examine the sensitivity of the retrieval to the penalty functions. When the penalty terms were excluded in the cost function, we found that the algorithm converged much slower. A relative rms error of 33% was obtained after 100 iterations and 13% after 500 iterations. From this experiment, one can see the importance of including penalties in the cost function. This has been pointed out in our previous studies (Sun et al. 1991; Sun and Crook 1994) and in studies by other researchers (e.g., Thacker 1988; Zou et al. 1993).

The above tests indicate that if the data are perfect, meaning that the data are frequently spaced and have no error, the traditional technique can outperform the adjoint technique. This is because the traditional technique directly solves the model equations to find the exact solution of the temperature field, while the adjoint technique seeks an approximate solution by iteratively minimizing the difference between the model equations and the data. In reality, however, the data always contain error and have a limited sampling frequency. These imperfection of data can cause the exact solution from the traditional retrieval to fail to represent the true temperature, as will be seen in the next subsection.

b. Results with degraded velocity data

In the previous section, we tested the two retrieval methods on "perfect" data. In this section, we compare

the retrieval techniques with "imperfect" or degraded data, that is, data with a time interval similar to that of operational radars and data contaminated by errors. Table 1 lists all the experiments presented in this section. A brief description is given for each experiment. In the table, the letter "A" within the parentheses indicates that the retrieval experiment is conducted using the adjoint method, while the letter "T" denotes the traditional method. In the following, we will refer to the traditional retrieval as run T and the adjoint retrieval as run A if both retrievals are performed in one experiment. The first set of experiments is designed to test the performance of both methods with data available every 5 min. In the subsequent three subsections, we then examine and compare the performance of the retrieval methods when the velocity data are contaminated by various errors. In the last subsection, we test how the efficiency of the adjoint method can be improved by incorporating results from the traditional retrieval.

Unless otherwise stated, the results shown for the adjoint retrieval are those after 95 iterations (about 100 simulations). This number of iterations was chosen because the cost function levels out after 95 iterations for most of the experiments. Although it is possible to obtain a more accurate retrieval with more iterations, the gain is small compared to the cost. All the experiments conducted using the adjoint method use the observations as the first guess of the horizontal velocity fields and the zero field as the first guess of the buoyancy field. The first guess of the vertical velocity is given by integrating the continuity equation upwards. All the experiments presented in this section use an assimilation window in which two datasets (at the start and at the end of the window) are provided. Although using more datasets will generally improve the retrieval for both methods, it does not change our general conclusions. It should be noted that when more time levels are used, there are more ways in which the tendency terms can be estimated for the traditional technique. In our study, however, we have found that a least squares fitting (linear or quadratic) does not change the general characteristic in the traditional retrieval. Since our study is aimed at the initialization of numerical forecast models, the moving-frame technique (see Chong et al. 1983) is considered impractical due to its requirement of choosing the frame of reference for each individual case.

1) TEMPORAL SAMPLING FREQUENCY

One difference between the two retrieval methods is the approximation on which the computation of the time derivatives is based. When only two volumes of data are supplied, the adjoint method attempts to find a model evolution that fits the velocity data at the start and the end of the assimilation window with the smallest error (in the least squares sense), while the traditional method assumes a linear evolution in time. In this section, we compare the performance of the retrieval methods when the velocity data are spaced 5 minutes apart in time (at t = 17.5 min and t = 22.5 min). This data interval was used because it is typical of the volume interval for operational radars. It should be noted that the scan intervals can be much shorter than 5 min for many research radars. However, since our work is aimed at the forecasting of low-level winds, our interest is in operational radars (for example, WSR-88D radars). The first experiment, experiment F1, was conducted to test the performance of the traditional technique's "exact" method. The tendency terms were calculated by differencing the data at t = 17.5 min and t = 22.5 min, while the advection and mixing terms were calculated using the average. The relative rms error in the retrieved θ field using the "ex-

TABLE 1. Summary of retrieval experiments.

Data degradation	Experiment	Comments
5-min frequency	F1 (T)	Test the "exact" method
	F2 (T, A)	Test the "inexact" method and compare it with the adjoint technique
	F3 (T)	Test the retrieval when performed at end of the assimilation window
	F4 (T + A)	Both techniques used in one retrieval experiment
Random error	RE (T, A)	Compare the two techniques with various magnitudes of random errors
Spatially correlated error	S1 (T, A)	Uncorrelated error from grid point to grid point
	S2 (T, A)	Horizontally correlated error with a scale of four grid points
	S3 (T, A)	Horizontally correlated error with a scale of eight grid points
	S4 (T, A)	Horizontally and vertically correlated error with a scale of four grid points
Rotational error	R1 (T, A)	Errors are added to the interior excluding the sounding location
	R2 (T, A)	Errors are extended to the sounding location
	R3 (T, A)	Errors are extended to the boundary
Divergence error	D1 (T, A)	Errors are added to the interior excluding the sounding location
	D2 (T, A)	Errors are extended to the sounding location
	D3 (T, A)	Errors are extended to the boundary

act'' method is 66%. In experiment F2, run T, we used the ''inexact'' method and the error decreased to 44%. The retrieved θ field at $t = 20$ min are shown in Fig. 5a for experiment F1 and Fig. 5b for experiment F2 using the traditional technique. As mentioned previously, when the ''exact'' method is used, error in the data is accumulated as the buoyancy is summed from one boundary to the other. Since the ''inexact'' method uses a vertical derivative over $2\Delta z$ to calculate the buoyancy, it has a tendency to smooth out these errors in the velocity data. For the remainder of this paper, we use the ''inexact'' method when calculating the buoyancy with the traditional technique.

When the adjoint method was applied to the same velocity data at $t = 17.5$ min and $t = 22.5$ min in experiment F2, a relative rms error of 10% was obtained. The retrieved θ field at $t = 20$ min is shown in Fig. 5c. The θ field retrieved using the adjoint method has little difference compared to the control simulation. However, distinct errors can be observed in the θ field retrieved using the traditional method (see Fig. 5b). Most of the error appears at the leading edge of the gust front and on the surface. It is likely that this region experiences the most nonlinear evolution in time.

Experiment F3 was designed to test the performance of the traditional retrieval when an Euler-backward scheme was used, namely when the advection and mixing terms were calculated using data at the end of assimilation period. For forecasting purposes, it is usually desirable to retrieve initial conditions at the time of the most current data. It is found that the retrieval performed at $t = 22.5$ min, with a relative rms error of 113%, is significantly less accurate than when a centered difference is used. This result is consistent with that obtained by Crook (1994) (see Fig. 5 of that paper). In contrast, the buoyancy retrieved by the adjoint method is rather consistent throughout the assimilation period, with the smallest error at the end of the window.

When the velocity datasets are spaced further in time, the assumption of linearity becomes less valid. To further explore and compare the sensitivity of the two methods to the temporal sampling frequency, five tests were conducted with assimilation periods of 1, 2.5, 5, 7.5, and 10 min, respectively. The rms error in retrieval is plotted against the assimilation period in Fig. 6. As expected, the performance of the retrieval by the traditional method degrades significantly as the length of the assimilation window increases. In contrast, the retrieval by the adjoint method is less sensitive. Figure 6 also shows that the adjoint method outperforms the traditional method for periods greater than 2 min. When the length of assimilation is less than 2 min, linearity is a good assumption, thus the traditional retrieval has a better accuracy than the adjoint method with 95 iterations.

It is important to point out that in the above tests the velocity data do not contain any error. When the data contain error, the traditional method with a short assim-

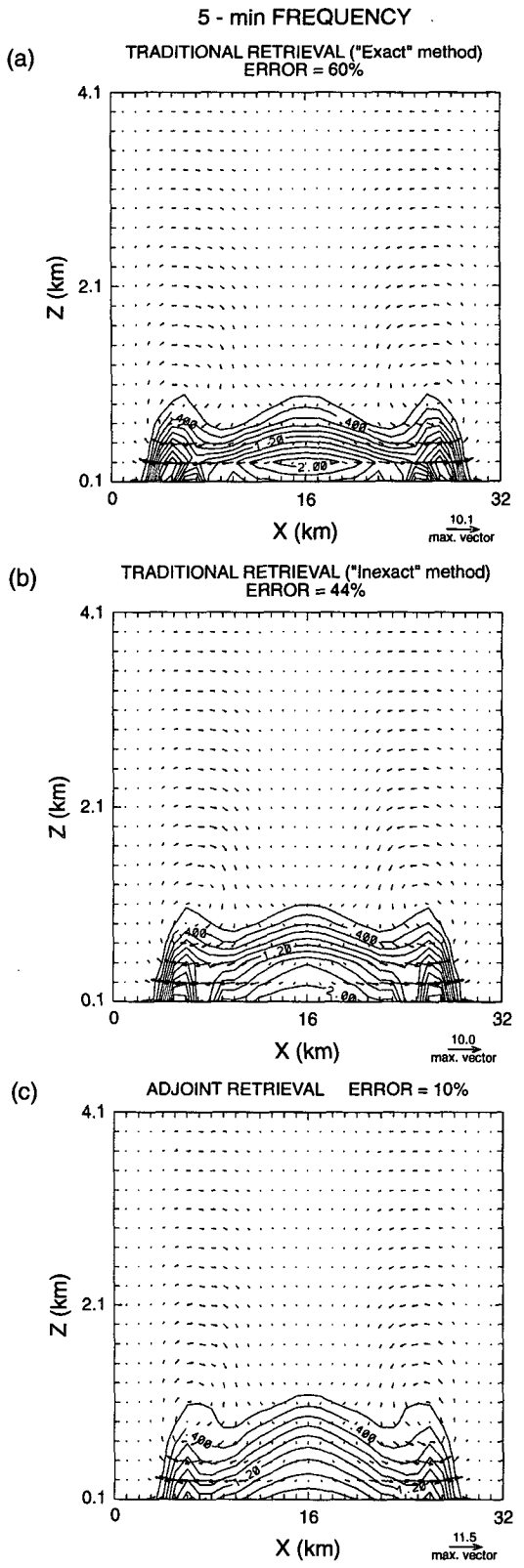

FIG. 5. Retrieved θ field from (a) experiment F1, (b) experiment F2 using the traditional technique, and (c) experiment F2 using the adjoint technique.

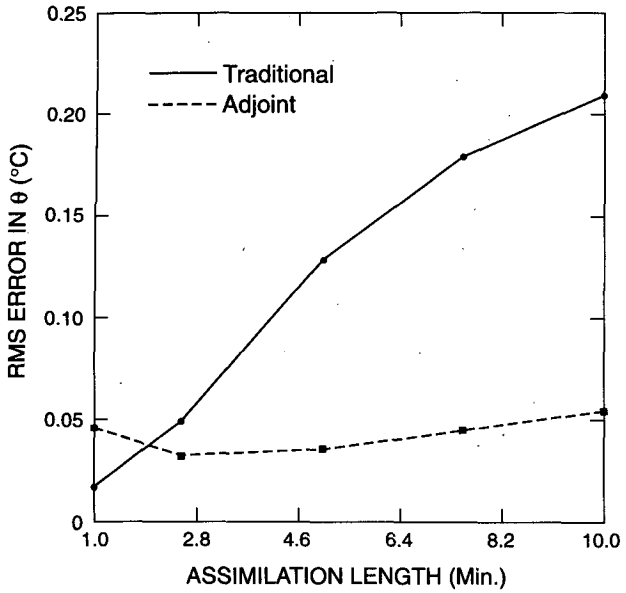

FIG. 6. The rms perturbation potential temperature error against length of assimilation. The solid curve represents the traditional method and the dashed curve represents the adjoint method.

ilation period may not work as well as in these tests since a short period can cause a large error in the tendency calculation.

2) RANDOM ERROR IN THE VELOCITY DATA

Previous studies have found that the traditional method is very sensitive to random velocity error (Hane et al. 1981; Crook 1994). In this section, we will examine the sensitivity of the adjoint retrieval to random errors in the velocity fields and compare it with the traditional retrieval. In experiment RE, random error in the range of ±0.0625, ±0.125, ±0.25, ±0.5, ±0.75, and ±1.0 m s^{-1} was added to the horizontal velocity fields at t = 17.5 min and t = 22.5 min in six tests. The results are compared in Fig. 7 by plotting the rms error in the retrieved buoyancy field against the magnitude of the velocity error. The dashed curve is for the adjoint retrieval, and the solid curve is for the traditional technique. It should be noted that the error in θ is calculated relative to the fields retrieved in experiment F2 (run T or run A), which use the same data interval of 5 minutes. Defining the buoyancy error in this way means that it vanishes as the velocity error goes to zero. As can be seen, the adjoint method has better performance at velocity errors of all magnitudes. The error in the retrieval for the traditional method exhibits a linear variation and exceeds 100% for velocity errors greater than ±0.5 m s^{-1}. Figure 8a and 8b show the retrieved θ fields from the traditional retrieval and the adjoint retrieval, respectively, using the noisy data with random error in the range of ±0.25 m s^{-1}.

A number of observational studies have shown that retrieval with the traditional technique can be improved by first smoothing the velocity data (see, for example, Lilly and Schneider 1991). To examine the effects of smoothing, we applied a three-dimensional filter to the input velocity data and then repeated the tests with the traditional method. The results are shown by the dot–dashed curve in Fig. 7. When the retrieval is performed after the velocity fields are smoothed, the retrieval improves for large errors but actually becomes worse for small errors. This is because smoothing can distort the signal such that it does more harm than good when the error is small. When larger error is contained in the fields, moderate smoothing can help suppress the noise and thus enhance the signal. Figure 8c shows the retrieval by the traditional method using the smoothed data. The rms error in Fig. 8c (60%) is reduced quite significantly from that in Fig. 8a (93%). However, it can be seen that distortion of the field has resulted from the smoothing on the velocity data.

3) SPATIALLY CORRELATED ERROR

In the previous section we have assumed that the velocity error is uncorrelated from grid point to grid point. Often the error in radar data is spatially correlated and may have different vertical and horizontal scales. To explore the sensitivity of the retrieval methods to spatially correlated errors, a set of experiments was conducted by varying the spatial structure of the error. In experiment S1, we added random error to the

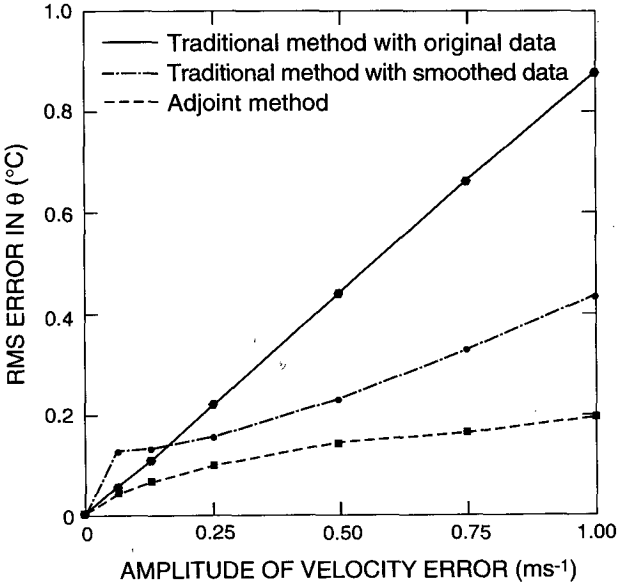

FIG. 7. The rms buoyancy error against maximum random error added to the velocity fields. The solid curve is for the traditional method, the dashed curve is for the adjoint method, and the dot–dashed curve is for the traditional method with smoothing applied to the velocity fields.

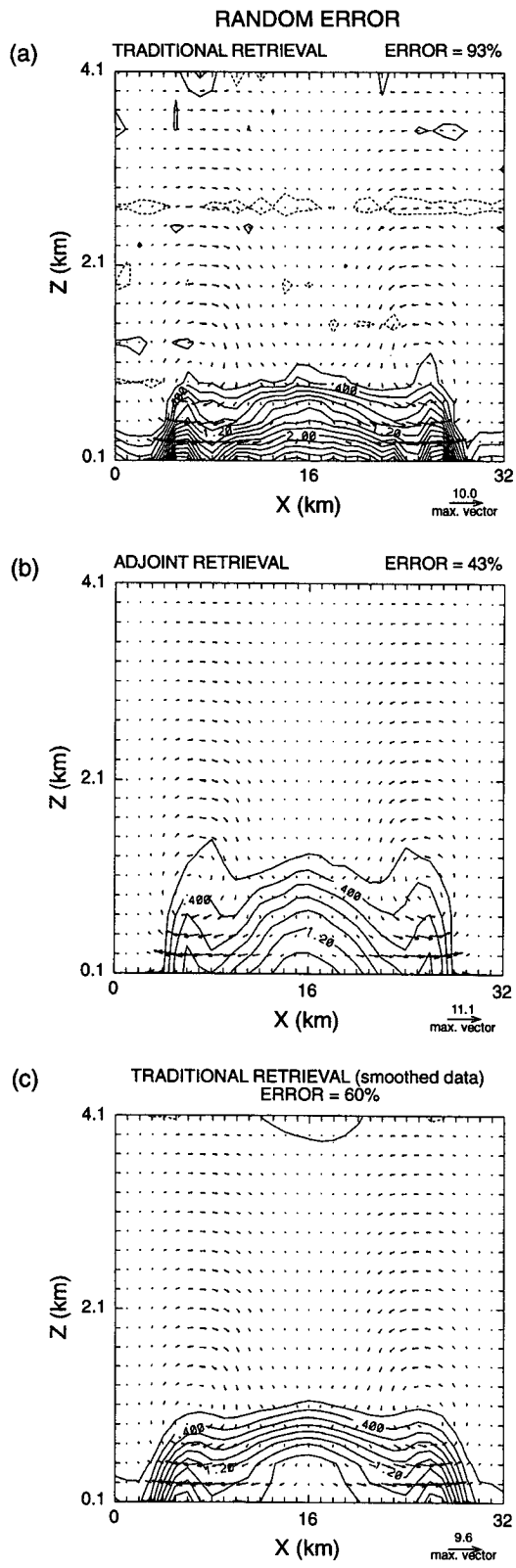

FIG. 8. The same as Fig. 5 but from experiment RE: (a) for the traditional method; (b) for the adjoint method; (c) for the traditional method with smoothing applied to the velocity fields.

horizontal velocity fields at each grid point (i.e., the same as experiment RE). In experiment S2, the random error was added to each grid point in the vertical and every fourth grid point in the horizontal, and then the error was linearly interpolated to the other grid points. Experiment S3 was similar to experiment S2, but the random error was given every eighth grid point in the horizontal. In experiment S4, the random error was given every fourth grid point both vertically and horizontally and the linear interpolation was applied in both directions. The linear interpolation serves to correlate the error in the direction it is applied. In all of the experiments, we adjusted the magnitude of the random error to produce an rms error of about 0.1 m s^{-1} in the velocity fields. Both retrieval techniques are tested in these experiments and their results are compared in Table 2. The adjoint method performs equally well in all experiments. However, the traditional method is quite case dependent. For experiments S1 and S4, the rms error in the retrieval is the same and reasonably small. For experiments S2 and S3, the error is quite large and the retrieved buoyancy is dominated by noise.

These results indicate that the traditional retrieval is very sensitive to the error that is correlated in the horizontal but uncorrelated in the vertical. When the error has similar characteristics in both the horizontal or vertical directions, the traditional retrieval appears to have a better performance. We explain this result in the following manner: the traditional retrieval solves the two-dimensional Poisson equation, (2.6), to first obtain the pressure field. When the velocity error is horizontally correlated, this error may bring about biases in the horizontal fields of F and G. Since F and G are related to the first derivatives of the pressure, the bias in F and G fields will produce bias in the pressure gradient field. When the pressure is adjusted to match the sounding pressure, this bias in the pressure gradient field will produce a bias in the pressure field. If the error is uncorrelated in the vertical, the pressure bias will oscillate from level to level. This oscillation will maximize the error in the vertical pressure gradient term $\partial p/\partial z$ and thus result in a large buoyancy error.

To further illustrate this point, the terms represented by G in (2.4) are summed over the horizontal domain for experiments S1, S3, and S4 with the traditional retrieval technique. The differences of ΣG between each experiment and the error-free experiment (experiment F2, run T) are calculated and plotted versus the vertical

TABLE 2. Summary of experiment 6.

	Description			
Experiment	S1	S2	S3	S4
Adjoint	0.16	0.14	0.17	0.13
Traditional	0.23	0.51	0.89	0.23

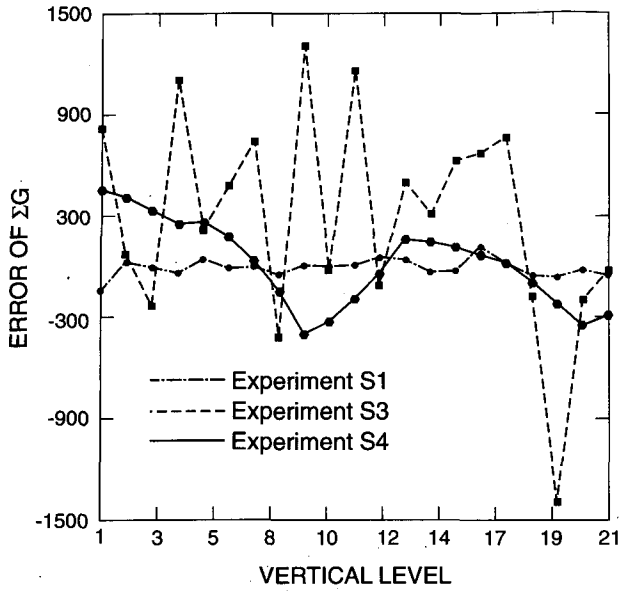

FIG. 9. Error of ΣG for experiments S1, S3, and S4 compared with experiment F2 (run T) plotted against vertical level. The dot–dashed curve is for experiment S1, the dashed curve is for experiment S3, and the solid curve is for experiment S4.

level in Fig. 9. For experiment S1, the difference is close to zero because the random errors cancel out as they are summed up. For experiment S3, there is clearly a bias in each level and the bias oscillates from one level to the next. When the velocity error is both correlated in the vertical and in the horizontal (experiment S4), there is bias in the forcing terms at each level, but the bias is correlated in the vertical.

Since the pressure field is obtained by solving a three-dimensional Poisson equation for the adjoint method, the above problem does not appear in the adjoint retrieval. This seems to be an advantage of the adjoint method over the traditional method.

4) ROTATIONAL AND DIVERGENT ERROR

In section 2a, we showed that the traditional technique responds differently to rotational and divergent error in the F and G fields. In this section, we compare the two retrieval techniques with rotational and divergent error. Because of the nonlinearity of the advection terms, the simplest method of adding rotational or divergent error to $[F, G]$ is to add the error through the tendency terms. We thus assumed a special form for the error field. A random function $\psi(x, y)$ was first given, and then if pure rotational error was required, the field $[\psi_y, -\psi_x]$ was calculated. This field was added to the horizontal velocity at $t = 22.5$ min and an equal, and opposite field was added to the velocity at $t = 17.5$ min. The total error added to the tendency terms was thus $2[\psi_y, -\psi_x]$ per 5 mins, while zero error was added to the advection and mixing terms since they are calculated using the average of the velocity fields at $t = 22.5$ and 17.5 min. For divergent error, the field $[\phi_x, \phi_y]$ was used and we also adjusted the error in the upper levels of the domain so that the vertical velocity vanished at the upper boundary. Term ϕ is also a random function, similar to ψ.

It should be noted that this special type of error is favorable to the traditional technique since the advection and mixing terms are calculated exactly, which is not necessarily the case with the adjoint method. With either divergent error or rotational error, we conducted three experiments and compared the two techniques in each experiment. We first added error only to the interior grid points but not the sounding location (experiment R1 for rotational error and experiment D1 for divergent error). We then extended the error to the sounding location (experiment R2 and experiment D2). Finally, we extended the error to the boundaries (experiment R3 and experiment D3). Table 3 lists the rms error in θ for these different experiments using each retrieval method. The rms error is computed against the retrieval from experiment F2 (run T or run A) in order to isolate the effect of error on the retrieval.

As shown in Table 3, the traditional method is able to retrieve the potential temperature field with zero error (compared to experiment F2, run T) when pure rotational error is added to the interior points but not the sounding location (experiment R1). With pure divergent error, however, it retrieves the θ field with an rms error of 0.28°C (experiment D1). When the adjoint method is applied to the same datasets, similar performances are obtained for both types of error (0.13°C in experiment R1 and 0.14°C in experiment D1).

When rotational error is extended to the sounding location, the buoyancy error remains at zero with the traditional method (experiment R2). Since the pressure is still retrieved exactly, no error has been introduced at the sounding location. However, when divergent error is extended to the sounding location, the error in θ increases substantially, from 0.28° to 0.46°C. As discussed in section 2a, the pressure retrieved at the sounding location with divergent error is $p_t + \phi$(i sound, j sound), where ϕ(i sound, j sound) is the value of the error function at the sounding location. The pressure at the sounding location is then adjusted back to p_t by subtracting ϕ(i sound, j sound) from the entire horizontal domain at that level. This adjustment

TABLE 3. The rms buoyancy error for the experiments with rotational error and divergent error.

	rms error in θ (°C)					
Method	R1	R2	R3	D1	D2	D3
Traditional	0.0	0.0	0.26	0.28	0.46	0.47
Adjoint	0.13	0.14	0.14	0.14	0.15	0.15

then adds further error to the pressure and buoyancy field.

When rotational error is extended to the boundaries, the buoyancy error increases from 0° to 0.26°C (experiment R3, run T). Although the rotational error still cancels out of the right-hand side of the Poisson equation (2.6a), now there is error in the boundary conditions (2.6b). When the divergent error is extended to the boundaries, the buoyancy error only increases slightly from 0.46° to 0.47°C. This is not surprising since divergent error at the boundary should only affect the pressure at the boundary, and hence the total buoyancy error should not increase significantly.

In contrast to the traditional method, the error in the retrieved potential temperature field using the adjoint method stays almost the same between the three experiments, either with rotational error or with divergent error. Since the adjoint method solves a three-dimensional Poisson equation, there is no need to specify a sounding location and to subtract the pressure at that location as done in the traditional technique. Furthermore, the adjoint method seeks an optimal fit between the model and the observations. The additional error extended to a particular point or to the boundaries does not change the optimal solution substantially.

These results suggest that the adjoint method is generally better at handling divergent error in $[F, G]$, while the traditional method may have an advantage with rotational error as long as that error does not extend to the boundaries. How this relates to error in the velocity fields is somewhat difficult to quantify because of the nonlinear terms in $[F, G]$. Results with gust fronts (Crook 1994) and convective storms (Hane et al. 1981) have suggested that the tendency terms usually dominate $[F, G]$. This means that the error that is predominantly divergent/rotational in the velocity fields will produce divergent/rotational error in $[F, G]$.

5) COMPARING THE VERTICAL VELOCITY FIELDS

A number of observational studies using the traditional radar analysis method (Ray et al. 1980; Gal-Chen and Kropfli 1984; Schneider 1991) have found that obtaining the vertical velocity by directly integrating the continuity equation can lead to unrealistically high velocities at the top of the integration domain. This occurs due to the fact that the error in the horizontal velocity fields is accumulated as the integration continues to the top. Various techniques (Ziegler 1978; Ray et al. 1980; Chong et al. 1983) were developed to overcome this difficulty so that a better-estimated vertical velocity can be obtained. Among them, the most commonly used technique was the variational adjustment technique developed by Ray et al. (1980). However, this technique was found to be numerically unstable by Schneider (1991) when applied to Phoenix II data. Since the vertical velocity obtained from the adjoint retrieval satisfies not only the continuity equation but also the equations of motion, the above-mentioned problem is avoided when the adjoint technique is used. In this section, we compare the vertical velocity obtained from the adjoint retrieval with that obtained from direct integration of the continuity equation. We use the results from experiment RE with the error magnitude of ± 0.50 m s^{-1} to make the comparison. Figure 10 shows the vertical velocity field from the control simulation (Fig. 10a), from the integration of the continuity equation (Fig. 10b), and from the adjoint retrieval (Fig. 10c). The rms error is 0.31 m s^{-1} from the integration of the continuity equation and 0.097 m s^{-1} from the adjoint retrieval. It is clearly seen that the vertical velocity field obtained from the adjoint retrieval is more accurate than that from the integration of the continuity equation. There is no accumulated noise in the upper levels of the domain and the strength of the updraft is closer to the control simulation.

6) ADJOINT RETRIEVAL WITH FIRST GUESS PROVIDED BY THE TRADITIONAL METHOD

In the previous subsections, we demonstrated that the adjoint method could, under most circumstances, retrieve the buoyancy field more accurately than the traditional method. In this section, we examine how the retrieval performs when both methods are combined. The easiest way to incorporate the two methods is to perform the traditional retrieval first and then use the results as the first guess to conduct an adjoint retrieval. This approach was used in experiment F4, in which the first guess of the potential temperature was that obtained by a traditional retrieval. The traditional retrieval was similar to that in experiment F2, run T, but the retrieval was performed at the start of the assimilation period using the Euler-forward scheme. The experiment was run for 100 iterations. The first-guess field for the potential temperature is shown in Fig. 11a. The relative rms error in θ is compared with that in experiment F2, run A, for each iteration in Fig. 11b. It can be observed in Fig. 11b that the error in experiment F4 reduces rapidly in the first ten iterations, equaling the accuracy achieved by experiment F2 after 50 iterations. We have also found that with this first guess, the penalty terms in the cost function are no longer needed, indicating that additional constraints are not necessary when a first guess contains sufficient information about the solution. This experiment suggests that the retrieved buoyancy field using the traditional method provides some important information, although it contains a large amount of error (90%). With this improved first guess, the adjoint method is able to obtain a rather accurate retrieval within ten iterations.

5. Summary and conclusions

We tested and compared the performance of the traditional method and the adjoint method in thermody-

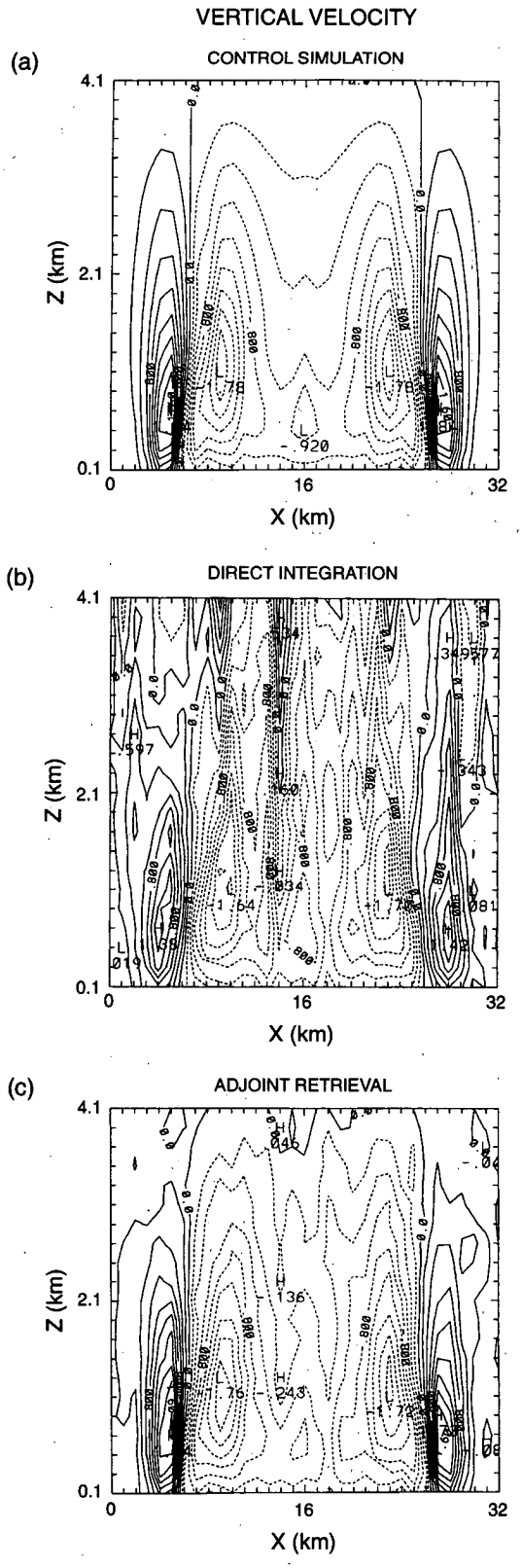

FIG. 10. Vertical velocity field (a) from control run, (b) from vertical integration of the continuity equation, and (c) from adjoint retrieval.

namic retrieval using both real data of a gust front and simulated data of a collapsing cold pool. In the real data tests, the adjoint method retrieved a smoother and more intense gust front. With simulated data, we first examined the sensitivity of the techniques to temporal resolution of the data and then compared the performance of the techniques when the velocity data were contaminated by errors with various structures. It is found that the adjoint method outperforms the traditional method in most of the cases examined. Other specific results from the simulated data study are summarized as follows.

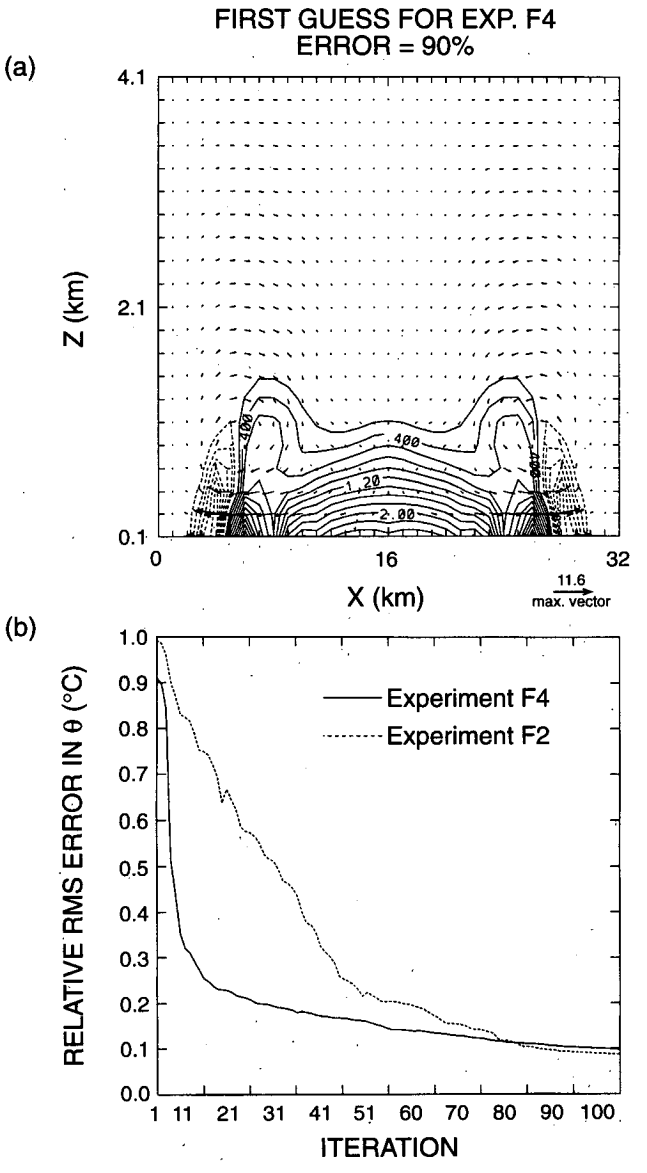

FIG. 11. (a) The first-guess field for potential temperature in experiment F4; (b) Relative rms error in θ against the number of iterations. The solid curve is for experiment F4 and the dotted curve is for experiment F2 (run A).

1) The adjoint method obtained a more accurate retrieval of the buoyancy field when the interval of the radar volumetric data was over 2 min. The adjoint retrieval showed little sensitivity to data frequency, while the traditional retrieval degrades significantly as the data interval increases.

2) As random error is added to the velocity data, the adjoint technique is able to produce a more accurate retrieval than the traditional technique with or without smoothing of the velocity data.

3) The adjoint technique is robust to various errors, while the traditional technique is sensitive to the error characteristic. When the error is correlated in the horizontal but not correlated in the vertical, the traditional technique gives poor results in the retrieved buoyancy.

4) The traditional method may have an advantage with rotational error in the terms $[F, G]$ as long as that error is confined to the interior, while the adjoint method is generally better at handling divergent error.

5) The traditional retrieval is sensitive to the velocity error at the sounding location. This problem does not appear in the adjoint retrieval because it is not necessary to specify the location of the sounding for the adjoint technique.

6) When errors exist in the horizontal velocity fields, a more accurate vertical velocity field can be obtained with the adjoint technique than the direct integration of the continuity equation.

7) When the two techniques are combined, that is, the initial guess in the adjoint retrieval is provided by the traditional technique, the efficiency of the adjoint method is improved significantly. A rather accurate retrieval can be obtained within 10 iterations.

There are two reasons why the adjoint method is more tolerant to error in most cases. First, the adjoint method retrieves the buoyancy field by fitting the model to the data rather than by directly inserting the velocity data into the model and assuming an evolution as done with the traditional method. Second, by solving a three-dimensional Poisson equation, the adjoint method is able to obtain a smoother three-dimensional pressure field than the traditional method in which a two-dimensional Poisson equation is solved first and then $\partial p/\partial_z$ is calculated to retrieve the buoyancy field.

Experiments using simulated data allow us to assess the performance of the retrieval methods more easily because the correct fields are known. It is therefore convenient to compare the sensitivity of the two methods with respect to various factors. However, it should be kept in mind that the simulated data can never replicate the complex atmospheric situations, although we have made every effort to have the simulated data resemble the real data. Although we have compared these two methods using a real dataset in our current study, the comparison is not considered complete until more tests are conducted on real data under various atmospheric conditions.

In the current study, we have focused our attention on the dry boundary layer. Recently we have extended the adjoint model to include moist processes and we are testing the technique on real data as well as simulated data. The aim is to retrieve the microphysical variables as well as the thermodynamic fields. Traditional methods for microphysical retrieval generally use the steady-state assumption, which can be a serious problem if a storm evolves rapidly with time. The adjoint technique is able to account for the time variation of the model variables. Moreover, it can retrieve the dynamical and microphysical variables simultaneously, allowing feedbacks between all processes. Preliminary tests of the adjoint technique on moist convection observed during the Convection and Precipitation/Electrification Experiment (CaPE) (Sun et al. 1995) have shown promise. Further tests of the technique in dynamical and microphysical retrieval are currently under way.

Acknowledgments. This research is sponsored by the National Science Foundation through an Interagency Agreement in response to requirements and funding by the Federal Aviation Administration's Aviation Weather Development Program. The views expressed are those of the authors and do not necessarily represent the official policy or position of the U.S. government. We would like to thank Drs. Jimy Dudhia and Xiaolei Zou for reviewing this paper.

REFERENCES

Arakawa, A., and V. R. Lamb, 1977: Computational design of the basic dynamical processes of the UCLA general circulation model. *Methods of Computational Physics, Vol. 17,* Academic Press, 174–265.

Chong, M., J. Testud, and F. Roux, 1983a: Three-dimensional wind field analysis from dual-Doppler radar data. Part II: Minimizing the error due to temporal variation. *J. Climate Appl. Meteor.,* **22,** 1216–1226.

——, ——, and ——, 1983b: Three-dimensional wind field analysis from dual-Doppler radar data. Part III: The boundary condition: An optimum determination based on a variational concept. *J. Climate Appl. Meteor.,* **22,** 1216–1226.

Courtier, P., 1985: Experiments in data assimilation using the adjoint model technique. *Workshop on High-Resolution Analysis,* UK, ECMWF, 1–20.

——, and O. Talagrand, 1987: Variational assimilation of meteorological observations with the adjoint equation. Part I: Numerical results. *Quart. J. Roy. Meteor. Soc.,* **113,** 1329–1347.

——, and ——, 1990: Variational assimilation of meteorological observations with the direct and adjoint shallow-water equations. *Tellus,* **42A,** 531–549.

Crook, N. A., 1994: Numerical simulations initialized with radar-derived winds. Part I: Simulated data experiments. *Mon. Wea. Rev.,* **122,** 1189–1203.

——, and J. D. Tuttle, 1994: Numerical simulations initialized with radar-derived winds. Part II: Forecasts of three gust front cases. *Mon. Wea. Rev.,* **122,** 1214–1217.

——, and R. Cole, 1994: Numerical forecasting of winds in the terminal environment. NCAR Tech. Note, NCAR/TN–406+STR.

Derber, J. C., 1985: The variational 4-D assimilation of analyses using filtered models as constraints. Ph.D. thesis, University of Wisconsin–Madison, 142 pp.

Gal-Chen, T., 1978: A method for the initialization of the anelastic equations: Implications for matching models with observations. *Mon. Wea. Rev.*, **106,** 587–606.

——, and R. A. Kropfli, 1984: Buoyancy and pressure perturbation derived from dual-Doppler radar observations of the planetary boundary layer: Applications for matching models with observations. *J. Atmos. Sci.*, **41,** 3007–3020.

——, and J. Zhang, 1993: On the optimal use of reflectivities and single Doppler radar velocities to deduce 3D motions. *Proc. of 26th Int. Conf. on Radar Meteorology,* Norman, OK, Amer. Meteor. Soc., 414–416.

Gill, P. E., W. Murray, and M. H. Wright, 1981: *Practical Optimization.* Academic Press, 401 pp.

Hane, C. E., and B. C. Scott, 1978: Temperature and pressure perturbations within convective clouds derived from detailed air motion information: Preliminary testing. *Mon. Wea. Rev.*, **106,** 654–661.

——, R. B. Wilhelmson, and T. Gal-Chen, 1981: Retrieval of thermodynamic variables within deep convective clouds: Experiments in three dimensions. *Mon. Wea. Rev.*, **109,** 564–576.

Hauser, D., and P. Amayenc, 1986: Retrieval of cloud water and water vapor contents from Doppler radar data in a tropical squall line. *J. Atmos. Sci.*, **43,** 823–838.

Laroche, S., and I. Zawadsky, 1993: Echo tracking by three variational analysis methods. *Proc. 26th Int. Conf. on Radar Meteorology,* Norman, OK, Amer. Meteor. Soc., 438–440.

Le Dimet, F. X., 1982: A general formalism of variational analysis. CIMMS Report, No. 22, 1–34.

——, and O. Talagrand, 1986: Variational algorithms for analysis and assimilation of meteorological observations: Theoretical aspects. *Tellus,* **38A,** 97–110.

Lewis, J. M., and J. C., Derber, 1985: The use of adjoint equations to solve a variational adjustment problem with advective constraints. *Tellus,* **37A,** 309–322.

Lilly, D. K., and J. M. Schneider, 1991: Dual Doppler measurement of momentum flux in the convective boundary layer: Phoenix II results. *Proc. of 25th Int. Conf. on Radar Meteorology,* Paris, France, Amer. Meteor. Soc., 432–435.

Liu, D. C., and J. Nocedal, 1988: On the limited memory BFGS method for large scale optimization. Tech. Rep. NAM 03, Department of Electrical Engineering and Computer Science, Northwestern University, Evanston, IL, 26 pp.

Mueller, C. K., and R. E. Carbone, 1987: Dynamics of a thunderstorm outflow. *J. Atmos. Sci.*, **44,** 1879–1898.

Parsons, D. B., C. G. Mohr, and T. Gal-Chen, 1987: A severe frontal rainband. Part III: Derived thermodynamic structure. *J. Atmos. Sci.*, **44,** 1615–1631.

Qiu, C-J., and Q. Xu, 1992: A simple adjoint method of wind analysis for single-Doppler data. *J. Atmos. Oceanic Technol.*, **9,** 588–598.

Ray, P. S., C. L. Ziegler, and W. Bumgarner, 1980: Single- and multiple-Doppler radar observation of tornadic storms. *Mon. Wea. Rev.*, **108,** 1607–1625.

Roux, F., 1985: Retrieval of thermodynamic fields from multiple-Doppler radar data using the equations of motion and the thermodynamic equation. *Mon. Wea. Rev.*, **113,** 2142–2157.

Ruledge, S. A., and P. V. Hobbs, 1983: The mesoscale and microscale structure and organization of clouds and precipitation in mid-latitude cyclone. Part VIII: A model for the "seeder–feeder" process in warm-frontal rainbands. *J. Atmos. Sci.*, **41,** 2949–2972.

Schneider, J. M., 1991: Dual Doppler measurement of a sheared, convective boundary layer. Ph.D. thesis, University of Oklahoma, 134 pp.

Shapiro, S., S. Ellis, and J. Shaw, 1995: Single-Doppler velocity retrievals with Phoenix II data: Clear air and microburst wind retrievals in the planetary boundary layer. *J. Atmos. Sci.*, **52,** 1265–1287.

Sun, J., and N. A. Crook, 1994: Wind and thermodynamic retrieval from single-Doppler measurements of a gust front observed during Phoenix II. *Mon. Wea. Rev.*, **122,** 1075–1091.

——, D. W. Flicker, and D. K. Lilly, 1991: Recovery of three-dimensional wind and temperature fields from simulated single-Doppler radar data. *J. Atmos. Sci.*, **48,** 876–890.

——, N. A. Crook, and L. J. Miller, 1995: Retrieval of the dynamical and microphysical structure of convective storms in CAPE using a cloud model and its adjoint. *27th Conference on Radar meteorology.*

Talagrand, O., and P. Courtier, 1987: Variational assimilation of meteorological observations with the adjoint vorticity equation—Part I: Theory. *Quart. J. Roy. Meteor. Soc.*, **113,** 1311–1328.

Thacker, W. C., 1988: Fitting models to inadequate data by inforcing spatial and temporal smoothness. *J. Geophys. Res.*, **93,** 10 655–10 665.

Tuttle, J. D., and G. B. Foote, 1990: Determination of the boundary-layer airflow from a single Doppler radar. *J. Atmos. Oceanic Technol.*, **7,** 218–232.

Verlinde, J., and W. R. Cotton, 1993: Fitting microphysical observations of nonsteady convective clouds to a numerical model: An application of the adjoint technique of data assimilation to a kinematic model. *Mon. Wea. Rev.*, **121,** 2776–2793.

Wilson, J. W., and W. E. Schreiber, 1986: Initiation of convective storms by radar-observed boundary layer convergent lines. *Mon. Wea. Rev.*, **114,** 2516–2536.

Wurman, J., 1994: Vector winds from a single transmitter bistatic dual-Doppler network. *Bull. Amer. Meteor. Soc.*, **75,** 983–994.

Xu, Q., C.-J. Qiu, J.-X. Yu, H.-D. Gu, and M. Wolfson, 1993: Adjoint method retrievals of microburst winds from TDWR data. *Proc. 26th Int. Conf. on Radar Meteorology,* Norman, OK, Amer. Meteor. Soc., 433–434.

Ziegler, C. L., 1978: A dual-Doppler variational objective abalysis as applied to studies of convective storms. Master's thesis, University of Oklahoma, 115 pp.

——, 1985: Retrieval of thermal and microphysical variables in observed convective storms. Part I: Model development and preliminary testing. *J. Atmos. Sci.*, **42,** 1487–1509.

Zou, X., I. M. Navon, and J. Sela, 1993a: Control of gravity oscillations in variational data assimilation. *Mon. Wea. Rev.*, **121,** 272–289.

——, ——, and ——, 1993b: Variational data assimilation with moist threshold processes using the NMC spectral model. *Tellus,* **45A,** 370–386.